

Two Distinct Populations of Calcium Channels in a Clonal Line of Pituitary Cells

Abstract. *The whole-cell variant of the patch clamp technique was used to study calcium channels in GH3 cells. Two distinct populations of calcium channels, first recognized from their closing kinetics, were observed. The slowly closing channels are activated in a relatively negative voltage range and are inactivated within 100 milliseconds. They conduct barium and calcium about equally well. The fast closing channels are activated at more positive voltages, are not inactivated during a 100-millisecond pulse, conduct barium in preference to calcium, and are activated slightly more rapidly than the slowly closing channels.*

Calcium channels are widely distributed and have significant roles in cell function. They inject calcium into cells that secrete by exocytosis (1), and they probably take part in pacemaking in cells that are autorhythmic (2). These quite different roles may not be served by a single set of calcium channels, and there is evidence for the existence of more than one type (3-7). Major alterations of calcium channel activity occurred in GH3 cells when a calcium solution was replaced with a barium solution (8). We have examined channel activity in the two solutions and provide clear kinetic evidence for the existence of two populations of calcium channels in a single cell type [see (9)]. The two populations, which we call fast deactivating (FD) and slow deactivating (SD) channels, differ from each other in at least five properties. The FD channels seem well suited for calcium injection, whereas the SD channels have properties that may qualify them for a role in pacemaking.

GH3 cells (derived from a rat pituitary adenoma) were obtained from American Type Culture Collection and maintained by standard procedures. The whole-cell patch clamp technique (10) was used to apply a voltage clamp to the cells (8). To improve the frequency response of the clamp, we used low-resistance patch pi-

pettes and a low-feedback resistor on the current-to-voltage converter. Sodium current was suppressed by substituting tris⁺ for Na⁺ and by adding tetrodotoxin (TTX). The solution referred to as "10 Ca" contained 10 mM CaCl₂, 150 mM tris-Cl, and 200 nM TTX, (pH 7.0). The 5 Ba and 10 Ba solutions were similar but with BaCl₂ substituted for CaCl₂. Potassium currents were eliminated by filling pipettes with cesium salts. The pipette contents rapidly equilibrated with the cell interior (8). The internal solution (in millimoles per liter) was 105 CsCl, 25 CsF, 20 EGTA, and 10 Hepes (pH 7.3).

The calcium channel activity of a GH3 cell is illustrated in Fig. 1. The channels were opened by a change in voltage from -80 mV to +20 mV (first arrow) and were closed by the return to -80 mV (second arrow). The magnitude of the current reflects the number of open channels and the electrochemical force driving ions through the channels. When the voltage is changed to +20 mV, the number of open channels increases and reaches a stable maximum in 3 or 4 msec. Repolarization to -80 mV increases the driving force for ion movement, causing a large jump in current magnitude. The "tail" current then decays in two phases as the calcium channels close. The fast phase is relatively

small and has a time constant of 110 μ sec. The time constant of the slow phase is 2.7 msec.

Barium moves through calcium channels as well as or better than calcium itself (11). Figure 1B was recorded after the solution was changed from 10 Ca to 10 Ba. The magnitude of the current during the pulse is about twice as great in barium as in calcium, and the fast phase of the current tail is substantially increased. This suggests that the channels responsible for the fast component have about a 2:1 selectivity for Ba²⁺ over Ca²⁺. The slow phase of the tail is about the same in the two solutions. All changes were completely reversed on returning to 10 Ca.

Are the components of tail current in Fig. 1, A and B, indeed the result of two channel types as the selectivity experiment suggests, or do they represent complex behavior of a single channel type? This question was addressed by the following experiments. The components can be separated from each other by prolonging the depolarizing pulse and inactivating the slow component. Figure 2 illustrates the tails at the end of a depolarization to +20 mV for the intervals shown next to each trace. The 6-msec tail has two distinct components as in Fig. 1. As the pulse duration is increased, the slow component becomes progressively smaller and is almost absent after 101 msec of depolarization. The fast component is about the same size in all the traces.

The two components were studied more quantitatively in two ways. In the first method, the 101-msec tail was assumed to give a relatively pure representation of the fast component and was subtracted from the tails recorded after 6- and 21-msec pulses. The remainder (Fig. 2B) was the isolated slow compo-

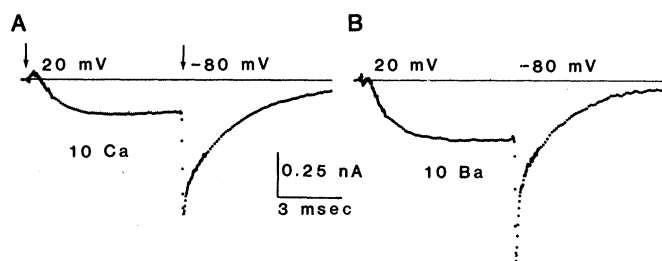


Fig. 1. Membrane currents reflecting calcium channel activity in a GH3 cell. (A) The cell was in 10 Ca, with Cs⁺ injected internally to suppress the potassium current. At the first arrow, the cell was depolarized to +20 mV and returned to -80 mV at the second arrow. The current reflects the flow of Ca²⁺ ions into the cell and is plotted with inward current negative. The tail current that follows the second arrow decays in two phases. (B) Channel activity with 10 Ba as the external solution. The same pulse procedure was used as in (A). The fast component of the tail current is enhanced. Temperature, 19°C.

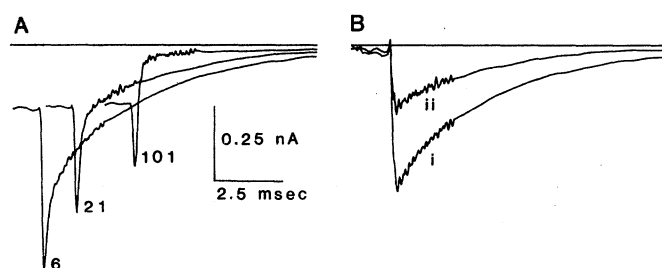


Fig. 2. (A) Closing of calcium channels after activating pulses lasting 6, 21, and 101 msec. The cell was in 10 Ba. The amplitude of the slow component is very small after a 101-msec activating pulse. (B) Fast and slow components separated by subtraction. The 101-msec trace is almost purely fast component. When the 101-msec tail is subtracted from the 6- and 21-msec tails, the remainder is a single slow exponential with a time constant of 3.3 msec for both the 6-msec tail (trace i) and the 21-msec tail (trace ii). Temperature, 18°C (see Table 1).

Table 1. Current tails from an experiment at 12°C, similar to that shown in Fig. 2, were fitted by the sum of two exponentials, which were extrapolated to the instant of repolarization.

Pulse duration (msec)	Fast component		Slow component	
	Amplitude (nA)	Time constant (μ sec)	Amplitude (nA)	Time constant (msec)
21	0.76	377	0.37	13.0
71	0.81	346	0.22	13.0
201	0.80	304	0.08	14.6

ment, a single exponential with the same time constant (3.3 msec) for both the 6-msec pulse (trace i) and the 21-msec pulse (trace ii). The 21-msec tail is smaller because of inactivation.

In the second method, tails recorded at 12°C were fitted by the sum of two exponentials. Kinetics are slower at 12°C, making it possible to record the fast component more faithfully (Table 1). The fast exponential had approximately the same amplitude (extrapolated to the beginning of the step) and the same time constant for pulses lasting 21 to 201 msec. The slow exponential, in contrast, diminished from 0.37 nA after 21 msec to 0.08 nA after 201 msec, but its time constant did not change significantly.

Tails after short pulses thus reflect fast and slow closing of channels. The slow phase is inactivated as the pulse is prolonged, and the fast phase remains unchanged. This is most easily explained by postulating that there are two channel types. One type (SD) closes slowly on repolarization and is inactivated during a long depolarization. The other type (FD) closes rapidly and is not inactivated during a 100-msec step. It is not impossible that these components represent two modes of behavior of a single channel type, as discussed below.

Inactivation provides a tool for separating the activity of the two channels and has been used to define the properties of the channels separately. Trace i of Fig. 3A is the current during depolarization to +30 mV and after return to -80 mV. The tail has obvious fast and slow components, reflecting activity of FD and SD channels. Trace ii was recorded during a similar pulse, but there was a previous 100-msec pulse to +20 mV that ended 5 msec before the trace begins. The earlier pulse inactivated the SD channels, and the slow phase is consequently absent in the tail. Current during the pulse diminished only slightly, indicating that most of the pulse current was carried by the FD channels. The tail currents might lead one to expect a larger change in pulse current after inactivation of the SD channels. The fast component is attenuated by the limited frequency response of the clamp and is much

larger when extrapolated to the beginning of the step.

The two channels are activated in different voltage ranges (Fig. 3B). Amplitudes of the fast and slow components of the tail were determined after 15-msec activating pulses and are plotted (normalized) as a function of activation voltage. The curve for the slow component lies about 20 mV to the left of the fast curve. The SD channels thus have a lower (more negative) threshold than the FD channels.

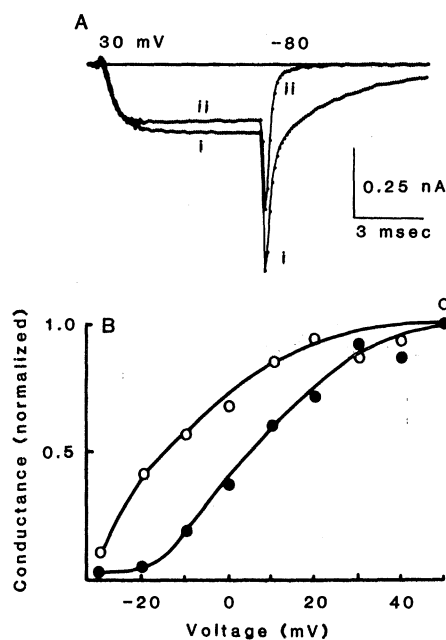


Fig. 3. (A) Separation of FD and SD channels by inactivation. Trace i shows the calcium current for a pulse to +30 mV in 5 Ba. Both FD and SD channel activity is evident in the tail. Trace ii was recorded after a conditioning pulse that inactivated the SD channels. The conditioning pulse, to +20 mV for 100 msec, was followed by a 5-msec period at -80 mV. Temperature, 21.7°C. (B) Conductance-voltage curves for FD and SD channels. Current tails following pulses to a number of voltages were each fitted by the sum of two exponentials. The curves are plots of the amplitudes of the slow (open circles) and fast (closed circles) components normalized relative to their maximum value. The threshold for SD channel activation is about 20 mV more negative than for FD channels. Almost identical results were obtained by directly measuring the maximum amplitude of the fast component after subtracting the fitted slow component, a procedure that minimizes extrapolation error.

The two channel types thus differ with regard to activation range, activation and deactivation kinetics, presence or absence of inactivation, and selectivity. Other experiments show that FD channel activity decreases significantly within 20 minutes after breaking into the cell (10), while SD channel activity is maintained. The activity of the FD channel is thus labile in our experimental conditions. If the two channel types have similar conductances in barium, there must be substantially more FD than SD channels.

Calcium channel activity can be modified by Bay K 8644, which prolongs the lifetime of the channel (12). This raises the possibility that we are observing two modes of behavior of a single channel type and that channels convert from one mode to the other even in the absence of a drug. We have seen nothing to support this idea, although it cannot be ruled out definitively. Instead, the SD channels behave as a stable population of fixed size for an extended period after breaking into the cell, usually until the seal between pipette and cell is lost. Activity of FD channels tends to disappear, but this never results in an increase in SD activity. Nor does inactivation of SD channels alter FD activity. Thus, our data is best explained by postulating two separate populations of calcium channels. If conversion from one type to the other occurs, it is precluded by our experimental conditions or occurs on a time scale that is long compared to our examination of a cell.

It is interesting to speculate on the role of these two types of calcium channels in the economy of a GH3 cell. Two behaviors of these cells that may be related to calcium channels are pacemaking and secretion. GH3 cells are autorhythmic, and they spontaneously generate action potentials at a rate that is increased by thyrotropin-releasing hormone. It has been suggested that calcium channel activity is involved in the pacemaker activity of GH3 cells (13). If so, it seems clear that the SD channels with their negative activation range are best suited to this role. GH3 cells secrete prolactin, probably as a result of the electrical activity in their membranes. If, as at the motor end plate, secretion is triggered by the entry of Ca^{2+} , both SD and FD channels may inject Ca^{2+} and thus play a role in stimulus-secretion coupling.

C. M. ARMSTRONG
D. R. MATTESON

Department of Physiology,
University of Pennsylvania
School of Medicine,
Philadelphia 19104

References and Notes

- B. Katz and R. Miledi, *J. Physiol. (London)* **192**, 407 (1967).
- A. Noma, H. Kotake, H. Irisawa, *Pflugers Arch.* **388**, 1 (1980).
- S. Hagiwara, S. A. Ozawa, O. Sand, *J. Gen. Physiol.* **65**, 617 (1975).
- R. Llinas and Y. Yarom, *J. Physiol. (London)* **315**, 549 (1981).
- A. P. Fox and S. Krasne, *Biophys. J.* **33**, 145a (1981).
- D. A. Nachshen and M. P. Blaustein, *J. Gen. Physiol.* **79**, 1065 (1982).
- M. C. Nowycky, A. P. Fox, R. W. Tsien, *Biophys. J.* **45**, 36a (1984).
- D. R. Matteson and C. M. Armstrong, *J. Gen. Physiol.* **83**, 371 (1984).
- _____, *Biophys. J.* **45**, 36a (1984).
- B. Sakmann and E. Neher, Eds., *Single Channel Recording* (Plenum, New York, 1983).
- S. Hagiwara and L. Byerly, *Annu. Rev. Neurosci.* **4**, 69 (1981).
- P. Hess *et al.*, *Biophys. J.* **45**, 394a (1984).
- P. S. Taraskevich and W. W. Douglas, *Proc. Natl. Acad. Sci. U.S.A.* **74**, 4064 (1977).

24 August 1984; accepted 25 October 1984

Peroxisomal Defects in Neonatal-Onset and X-Linked Adrenoleukodystrophies

Abstract. Accumulation of very long chain fatty acids in X-linked and neonatal forms of adrenoleukodystrophy (ALD) appears to be a consequence of deficient peroxisomal oxidation of very long chain fatty acids. Peroxisomes were readily identified in liver biopsies taken from a patient having the X-linked disorder. However, in liver biopsies from a patient having neonatal-onset ALD, hepatocellular peroxisomes were greatly reduced in size and number, and sedimentable catalase was markedly diminished. The presence of increased concentrations of serum pipecolic acid and the bile acid intermediate, trihydroxycoprostanic acid, in the neonatal ALD patient are associated with a generalized diminution of peroxisomal activities that was not observed in the patient with X-linked ALD.

Two distinct types of adrenoleukodystrophy (ALD) that differ in their age of onset and mode of inheritance have been identified. An X-linked form of ALD (Schilder's disease) usually appears in prepubertal boys and is characterized by progressive destruction of cerebral white matter and adrenal cortex. Death occurs during adolescence in most cases (1). A neonatal-onset (neonatal) form of ALD that is not X-linked has also been described (2). Affected children suffer from severe hypotonia and seizures and usually do not live longer than six years. Accumulations of very long chain fatty acids (C₂₆ and C₂₄) are characteristic of neonatal and X-linked types of ALD, and fibroblasts from patients with both forms of ALD are deficient in their ability to oxidize very long chain fatty acids (2-5).

The oxidation of some very long chain fatty acids appears to occur preferentially in peroxisomes (6). Therefore, we examined the morphological and biochemical properties of peroxisomes in liver biopsies from a 12-year-old boy with X-linked ALD and a 3-year-old girl with neonatal ALD (7). Abnormalities of cholic and chenodeoxycholic acid synthesis and pipecolic acid excretion were also investigated in these patients because bile acid intermediates (8) and pipecolic acid (9) accumulate in the serum and urine of infants with Zellweger's cerebro-hepato-renal syndrome (10), in which there are no detectable hepatic peroxisomes.

The hepatic architecture was normal

in the biopsies from both patients; however, portal connective tissue was increased in the liver of the patient having the neonatal disease. There were striking differences in the size, number, and configuration of hepatocellular peroxisomes in these two diseases. In the child with X-linked ALD, peroxisomes were abundant and normal in size, ranging from 0.25 to 0.75 μm in diameter in 39 electron micrographs photographed at a magnification of $\times 19,500$ to $\times 37,500$ (11). The peroxisomes had a characteristic coarsely fibrillar, moderately electron-opaque matrix and were often found in clusters (Fig. 1A). In the patient with neonatal ALD, peroxisomes were sparse, scattered, and small and, when measured in 62 electron micrographs, had diameters that ranged from 0.1 to 0.25 μm (12) (Fig. 1B). Sometimes their matrices were denser than normal and separated from the membranes.

There was a tenfold decrease in the

Table 1. Plasma hexacosanoic acid (C26:0) and ratio of C26:0 to docosanoic acid (C22:0). For ALD patients, the means of two determinations are shown (32). Mean \pm standard deviation in controls were derived from assays of 65 normal individuals. Quantitation of fatty acids was as described in (4).

Subject	C26:0 ($\mu\text{g}/\text{ml}$)	C26:0/ C22:0
X-linked ALD	1.278	0.075
Neonatal ALD	1.783	0.215
Control	0.33 \pm 0.18	0.014 \pm 0.076

number and mean volume of hepatocellular peroxisomes in the patient having neonatal ALD as compared to the patient having X-linked ALD (13). The mean peroxisomal volume in the X-linked ALD child was 0.070 μm^3 . In the neonatal ALD patient, total peroxisomal volume per hepatocyte was 1 percent of that observed in the liver of the X-linked disease patient. Anucleoid peroxisomes (0.07 to 0.20 μm in diameter) were also present in the intestinal epithelium of the patient with neonatal ALD (Fig. 1C); these resemble normal intestinal peroxisomes in size and shape (11, 12).

In the neonatal ALD patient, lysosomal and cytoplasmic inclusions composed of parallel lamellae (2.5 to 5 nm in thickness) were common in Kupffer cells (Fig. 1D). These lamellae are similar to those described as containing cholesterol esters with very long fatty acid chains after extraction in propylene oxide (3). Plasma concentrations of the very long chain fatty acid hexacosanoic acid (C26:0) were elevated and the ratios of C26:0 to docosanoic acid (C22:0) were abnormal in both patients (Table 1).

Hepatic catalase activity (14) in the X-linked ALD patient was normal. Moreover, as in two controls, half of the catalase could be sedimented under centrifugation conditions where peroxisomes, but not soluble catalase, are pelleted (Table 2). This indicates that at least half of the catalase was in peroxisomes; the balance may have been located in the cytosol or may have been released from peroxisomes damaged during homogenization. In contrast, the neonatal ALD patient had a low liver catalase activity of which only 12 percent was sedimentable (Table 2). In absolute terms, sedimentable catalase was 4 percent of that of the X-linked ALD patient. The specific activity of catalase in the intestinal mucosa of the neonatal ALD patient was 68 milliunits (mU) per milligram of protein. In two controls, the catalase-specific activities were 44 mU per milligram of protein.

The peroxisomal β -oxidation capacity of the X-linked ALD patient's liver, assayed with palmitoyl-coenzyme A (palmitoyl CoA) as substrate (15), was 1.4 nmol/min per milligram of protein. This may be compared with a value of 0.96 nmol/min per milligram of protein that we observed on an adult control, and with a published normal human value of approximately 1 nmol/min per milligram of protein (16).

Increased concentrations of pipecolic acid (17) were found in serum samples of the neonatal ALD patient at 2 and 3 years of age (87 nmol/ml; control, 5